Biomaterials Science

ROYAL SOCIETY OF CHEMISTRY

PAPER

View Article Online
View Journal | View Issue

Check for updates

Cite this: *Biomater. Sci.*, 2024, **12**, 3458

Chitosan-based multifunctional oxygenating antibiotic hydrogel dressings for managing chronic infection in diabetic wounds†

Shahrzad Abri,[a] Hannah Durr,[b] Hazel A. Barton,[c] Kayla Adkins-Travis,[d] Leah P. Shriver,[d,e,f] Dipak D. Pukale,[a] Judith A. Fulton[g,h] and Nic D. Leipzig *[a,b]

Current treatment strategies for infection of chronic wounds often result in compromised healing and necrosis due to antibiotic toxicity, and underlying biomarkers affected by treatments are not fully known. Here, a multifunctional dressing was developed leveraging the unique wound-healing properties of chitosan, a natural polysaccharide known for its numerous benefits in wound care. The dressing consists of an oxygenating perfluorocarbon functionalized methacrylic chitosan (MACF) hydrogel incorporated with antibacterial polyhexamethylene biguanide (PHMB). A non-healing diabetic infected wound model with emerging metabolomics tools was used to explore the anti-infective and wound healing properties of the resultant multifunctional dressing. Direct bacterial bioburden assessment demonstrated superior antibacterial properties of hydrogels over a commercial dressing. However, wound tissue quality analyses confirmed that sustained PHMB for 21 days resulted in tissue necrosis and disturbed healing. Therefore, a follow-up comparative study investigated the best treatment course for antiseptic application ranging from 7 to 21 days, followed by the oxygenating chitosan-based MACF treatment for the remainder of the 21 days. Bacterial counts, tissue assessments, and lipidomics studies showed that 14 days of application of MACF-PHMB dressings followed by 7 days of MACF dressings provides a promising treatment for managing infected non-healing diabetic skin ulcers.

Received 8th March 2024,
Accepted 25th May 2024

DOI: 10.1039/d4bm00355a

rsc.li/biomaterials-science

Introduction

Non-healing chronic wounds associated with diabetes mellitus present a major challenge to patients and the healthcare system.[1,2] Bacterial infection in these wounds is common, often leading to progressive systemic infection and limb amputation.[3] This challenge can be further exacerbated by diabetic angiopathy and ischemia, which limit oxygen and supply of nutrients to the site of injury, leading to inflammation and increased risk of infection.[4,5] Combating diabetic wound infections is often achieved *via* systemic and/or local antibiotic therapy to treat or prevent infections.[6]

Considering the growing problem of multidrug resistance in bacteria, selecting an appropriate antibacterial treatment for infected non-healing wounds is challenging. This issue is highlighted for pathogenic bacterial strains such as *Pseudomonas aeruginosa*, due to their intrinsic resistance to antibiotics.[7] Any long-term antibacterial treatment strategy must also consider that prolonged use of certain antibiotics can cause host tissue necrosis and inflammation, leading to chronic complications and further delayed wound healing.[8] Antiseptics, such as PHMB or silver compounds, are effective against a wide spectrum of bacteria, with a reduced likelihood of triggering resistance.[9] Nonetheless, use of antiseptics can be limited by their potential host toxicity towards cells essential to wound healing processes.[8] Topical delivery systems can alleviate this problem by controlling the delivery of antiseptics to the skin, preventing the drug from entering systemic circulation in large doses and, ultimately, limiting tissue necrosis.[10] As a result, the effectiveness of antiseptics for wound healing can be enhanced by encapsulating them into a carrier.

Many researchers, including our group,[11–18] have previously utilized oxygen-delivering platforms to improve wound healing leading to enhancement of oxidative wound healing. However,

[a]*Department of Chemical, Biomolecular, and Corrosion Engineering, The University of Akron, Akron, Ohio 44325, USA. E-mail: nl21@uakron.edu*
[b]*Integrated Biosciences Program, Department of Biology, The University of Akron, Akron, Ohio 44325, USA*
[c]*Department of Geological Sciences, The University of Alabama, Tuscaloosa, Alabama 35487, USA*
[d]*Department of Chemistry, Washington University in Saint Louis, Saint Louis, MO 63130, USA*
[e]*Center for Proteomics, Metabolomics, and Isotope Tracing, Washington University in Saint Louis, Saint Louis, MO 63130, USA*
[f]*Department of Medicine, Washington University in Saint Louis, Saint Louis, MO 63130, USA*
[g]*Summa Health System-Translational Research Center Akron, Akron, Ohio 44304, USA*
[h]*Northeast Ohio Medical University-REDIzone, Rootstown, Ohio 44272, USA*
† Electronic supplementary information (ESI) available. See DOI: https://doi.org/10.1039/d4bm00355a

to date there is limited research on wound oxygen therapies and their role in anti-infective strategies, especially in the form of easy-to-use oxygenating wound dressings. Oxygen availability is known to be important for host-driven antimicrobial responses for fuelling the production of ROS, while providing oxidative energy to upregulate the innate immune processes to combat infection.[19,20] It has also been reported that supplemental oxygen can synergistically improve the antimicrobial effects of certain antibiotics by enhancing their functionality and increasing drug susceptibility of pathogens through stimulating aerobic respiration[19,21] leading to an increased bacterial drug uptake and death.[21,22]

Therefore, with this motivation we designed an oxygenating controlled-release antibacterial platform *via* encapsulating PHMB antiseptic within our oxygenating perfluorocarbon methacrylamide chitosan (MACF) hydrogel sheet dressings. Chitosan, a naturally abundant carbohydrate, is the key component of our MACF-based wound dressing, imparting unique properties, such as antimicrobial activity, haemostatic properties, and ability to promote tissue regeneration and wound closure,[23,24] that contribute to the efficacy and wound healing benefits of our dressings.[19,20] For this study, we began with the hypothesis that chitosan would serve as a foundation for creating oxygenating MACF hydrogel sheet dressings against *Pseudomonas aeruginosa* infection and enhance wound healing processes in chronic diabetic dermal wounds. A main objective was to demonstrate that a chitosan-based oxygenating MACF dressing, encapsulating PHMB, provides superior anti-infective properties, accelerated wound closure, and reduced adverse effects compared to a commercial wound dressing (Kendall-PHMB). To achieve this, we created an infected chronic wound model challenged by *P. aeruginosa* in transgenic diabetic mice to evaluate the wound healing and anti-infective properties of our oxygenating and antibacterial dressings. Through comprehensive assessments, including bacterial bioburden measurements, lipidomic evaluations, and wound quality assessments, we demonstrated the potential of our innovative wound dressing to address the multifaceted challenges of infected non-healing diabetic ulcers. Lastly, upon discovering the detrimental effects of continuous PHMB antiseptic usage for 21 days, we aimed to enhance wound healing outcomes by optimizing the duration of PHMB application on our wound models and showed the advantages of a 14-day application of PHMB *via* MACF hydrogels through a series of wound quality assessments, lipidomic evaluations, and bacterial bioburden measurements.

Experimental

Materials and methods

Hydrogel synthesis. Oxygenated MACF dressings were prepared as described in our previous *in vivo* wound healing models[16,17,25] starting from purified chitosan (ChitoClear 43010, DDA ~80% M_w = 200 kDa, Primex, Siglufjörður, Iceland) to make MAC.[16,17,26–28] To make MACF, MAC was fluorinated by dropwise addition of a methanol-PFOC mixture (Sigma Aldrich) solution in a 48 hour reaction. The polymer was then dialyzed against DI water, freeze dried, and stored in airtight containers until further use.

To make the hydrogels, the corresponding polymer was dissolved in ultrapure water (3 wt%, 18 MΩ, Millipore, Billerica, MA, USA) and sterilized by autoclaving. Photo-crosslinker was prepared by dissolving hydroxycyclohexyl phenyl ketone in 1-vinyl-2-pyrolidone (both Sigma Aldrich) and added to polymer solution under sterile conditions (Final ratio: 0.9 mg photo-crosslinker per gram of polymer solution) and mixed *via* speed mixing (DAC 150 FVZ, Hauschild Engineering, Hamm, Germany) at 3000 rpm for 2 minutes. The polymer-photo initiator mixture was moulded in a six well plate (CELLSTAR, Greiner) to a liquid depth of 4 mm and UV-crosslinked for 4 minutes (using a UV-light source at 365 nm, Uvitron, West Springfield, MA). Hydrogels were then cut using a sterile 6 mm biopsy punch for use as wound dressings. Similar procedures were followed to make MAC-PHMB and MACF-PHMB dressings, except that PHMB (Musechem, Fairfield, NJ) was added to the polymer solution (0.5 wt%) before crosslinking. To perform the study, sterile MACF dressings (either with or without PHMB) were saturated with medical grade oxygen and kept inside a closed hypoxia chamber (Billups-Rothenberg, Inc., San Diego, CA) flushed with oxygen overnight. Oxygenation was repeated an hour before the dressing changes to ensure maximum oxygen saturation.

Hydrogel characterization experiments. Quantitative proton and fluorine NMR (^{1}H NMR and ^{19}F NMR, Varian 500 MHz) were used to identify the methacrylation degree and fluorination content, respectively. Polymers were dissolved in deuterated acetic acid (CD_3CO_2D) at 1 wt%. Percent methacrylation (DM%) and fluorine concentration (C_F) were calculated using eqn (1) and (2) below,[14] using the peak area at the mentioned chemical shifts (I_X).

$$\mathrm{DM}(\%) = 3 \times \left(\frac{I_{5.6} + I_{6.0}}{I_{2.8-4.0}}\right) \times 100 \quad (1)$$

Deuterated trifluoroacetic acid (d-TFA, Sigma Aldrich) was used as an internal standard (Cd-TFA = 1 nM) to calculate the concentration of fluorines (CF) in MACF using quantitative 19F NMR, based on the number of nuclei (N) for fluorine, as we have previously reported.[14,29]

$$C_F = \frac{I_F}{I_{\text{d-TFA}}} \times \frac{N_{\text{d-TFA}}}{N_F} \times C_{\text{d-TFA}} \quad (2)$$

To study the mechanical properties, circular hydrogels (diameter: 8 mm, thickness: 3–5 mm) were placed at the centre of the plate on a rheometer (TA Instruments ARES-G2 Rotational Rheometer). The experiment was conducted in linear mode, with a strain of 1% and a shear rate ranging from 1 to 100 rad s^{-1}. The frequency was increased by 5 rad s^{-1} and recorded using TRIOS software.

To test the swelling properties, hydrogels (with same dimensions as rheological analyses) were freeze-dried

(Labconco, Freezone 4.5 Liter Freeze Dry System) for 24 hours and weighed to record their dry mass (M_D). The freeze-dried hydrogels were re-hydrated in 3 mL of 1× PBS (pH 7.4) and incubated at 37 °C to initiate the swelling process. At specific time-points, gels were placed in a 40 μm cell strainer (Fisher Scientific, cat# 08-771-1) on a centrifuge tube, and briefly centrifuged at 1500 rpm for 60 seconds to remove any remaining surface PBS. The mass of the gels after swelling (M_S) was then recorded using an analytical balance (Sartorius ME235S). The swelling ratio (Q_M) was calculated as:

$$Q_M = \frac{M_s}{M_D} \quad (3)$$

To evaluate cell viability responses after direct contact with hydrogels (with or without PHMB), HDFs were seeded at a density of 2500 cells per cm^2 in 12 well plates. The cells were cultured in DMEM (high glucose, Sigma Aldrich), supplemented with 10% FBS (ThermoFisher Scientific) and 1% streptomycin/penicillin (ThermoFisher Scientific). Hydrogels including PHMB at concentrations of 0, 5, 10, 20, and 50 μg mL^{-1} were co-incubated with cells once the culture confluency reached approximately 75%. At specific time points, gels were removed and PrestoBlue™ Cell Viability Reagent (ThermoFisher Scientific) was added to the cells following the manufacturer's protocol. The fluorescence intensity of the cell supernatant was then recorded using a microplate reader (Tecan Infinite M200) with excitation and emission wavelengths of 560 nm and 590 nm, respectively. The same methodology was used to study the effect of direct contact with PHMB on the viability of HDFs.

Infected diabetic (*db*/*db*) mouse wound model. All animal experiments complied with the National Research Council's Guide for the Care and Use of Laboratory Animals and was overseen by the IACUC at the Northeast Ohio Medical University (NEOMED, Rootstown, OH). Adult, 8–12-week-old BKS.Cg-*Dock7*^{m} +/+ *Lepr*^{db}/J (*db*/*db*) homozygous mice were used in this study (Jackson Laboratory, Bar Harbor, ME). To consider the potential effect of sex on wound healing results, both male and female mice were included initially. All procedures involving live bacteria were performed aseptically inside a biosafety cabinet. To limit bacterial contamination, animals were single housed in micro-isolator cages equipped with HEPA filter tops. For the initial wounding surgery, under anesthesia using 2.5% isoflurane, animals' backs were shaved and disinfected using chlorhexidine and ethanol. Two sterile, clear, medical-grade silicone splints (12 mm outer diameter and 8 mm inner diameter) were placed on the animal's back at 10 mm caudal from the shoulder blades and 15 mm lateral from the midline and attached using Vetbond® tissue adhesive (3 M, Maplewood, MN) and five non-absorbable sutures (Ethicon, Raritan, NJ) per splint. Wounds were created at the center of the silicone rings using a 6 mm diameter biopsy punch to remove the first two layers of skin down through the panniculus carnosus. Ketoprofen (5 mg kg^{-1}) was given subcutaneously to the animals to provide 48–72 hours of pain relief the day of the surgery and the day after. A liquid culture of *Pseudomonas aeruginosa* (ATCC 15692, American Type Culture Collection, Manassas, VA) was used to infect wounds at 10^7 CFU mL^{-1} in PBS. The number of bacteria was confirmed by a dilution agar plate counting method and OD_{600}.[30] To induce infection, 80 μl of inoculum was introduced to the wound surface and allowed to establish for a 24 hour interval before starting any treatments. Animal study treatments included, oxygenated MACF (+/− bacteria), oxygenated MACF-PHMB (+/− bacteria), MAC (+/− bacteria), MAC-PHMB (+/− bacteria), and commercial PHMB dressing (Kendall-PHMB dressing, Cardinal Health, Inc., Dublin, OH) dressings and were randomly assigned to the wounds (two treatments per animal). A group of wounds infected with (Tegaderm (infected)) as well as a no-dressing group *P. aeruginosa* (Tegaderm (non-infected)) served as our controls. All wounds and treatments were covered with sterile Tegaderm (3M) dressings. Dressings were placed starting from day 1 after the surgery and were changed on days 3, 5, 7, 9, 11, 14, and 17. Animals were weighed, and their blood glucose was checked weekly using a glucometer (Medtronic, Minneapolis, MN) starting from surgery to confirm the diabetic status of the animals. The animals were sacrificed on day 21 *via* CO_2 exsanguination and cervical dislocation. Wound tissue samples were collected and preserved for further analyses.

Wound closure assessment. During the animal study, wounds were photographed at dressing change times using a digital camera (Canon EOS Rebel SL1, Tokyo, Japan) with a physical ruler as a measuring scale. The wound perimeter was traced for every image using ImageJ (National Institutes of Health [NIH], Bethesda, MA). Wound area values were normalized to original size for each treatment.

Wound histology. Upon harvest, wound tissue samples were excised using 8 mm biopsy punches and fixed using 4% paraformaldehyde solution in PBS at 4 °C overnight and stored in 70% ethanol. Samples were then processed, paraffin-embedded, and sectioned transversely (4 μm thickness). H&E and Masson's trichrome staining were used to assess wound epithelialization and collagen maturation.[17] The section images were then analyzed in terms of the length of the epithelial tongue from H&E and trichrome images using ImageJ. For open wounds, the edges of the newly formed epithelial tongue on both sides were considered as the wound margins.

Tissue gram staining. To identify the presence and morphology of bacteria (Gram positive or Gram negative), we used a Gram staining technique[31] on wound sections. Briefly, normal Gram-staining was applied to slides, followed by dehydrating, counterstaining in 6% alcoholic saffron (VWR) and mounting using Permount (Fisher Scientific). A slide scanner (BX61VS, Olympus) was used to image the slides at a magnification of 20×.

Quantitative polymerase chain reaction (qPCR). qPCR was used to quantify *P. aeruginosa* and overall bacterial load in wound tissues. Snap frozen fresh 1.5 mm biopsies of tissue or aqueous fractions from metabolomics extractions (see below) were completely homogenized in 1 mL of ddH_2O using motorized pestle and sterile pellet mixer (VWR). Genomic DNA was

extracted from homogenized samples using the Genomic DNA Purification Kit (Thermo Scientific™ GeneJET). DNA was plated in a 96 well qPCR plate with LightCycler® 480 SYBR Green I master mix (Roche Diagnostics), and forward and reverse primers (Thermo Scientific) specific for the 16S rRNA gene *for P. aeruginosa* or a general 16S rRNA gene for overall bacterial bioburden. Positive controls of genomic DNA from *P. aeruginosa* or *E. coli* and negative controls of ddH_2O in place of DNA were included. qPCR was run on a thermocycler (Roche Diagnostics) with a 2-minute initial denaturization at 95 °C, and 40 cycles of 20-second melt at 94 °C, 20-second annealing at 58 °C, and 40-second extension cycles at 72 °C. Fluorescence cycle threshold (Ct) values were quantified using Roche Diagnostics software and absolute quantification analysis. Absolute values were calculated on a bacterial concentration curve at OD_{600}.

Immunohistochemistry. A rat Ly-6G Alexa Fluor 647 primary antibody (1 : 200, Santa Cruz Biotechnology, Dallas, TX) was used to label neutrophils. A primary mouse CD68 (KP1) Alexa Fluor 546 antibody (1 : 200, Santa Cruz Biotechnology) was concurrently used to stain macrophages. Deparaffinized sections were subjected to heat antigen retrieval *via* tris-EDTA and 0.05% tween 20 for 8 minutes, followed by a rapid cooling on ice. Next, permeabilization was achieved using 0.1% Triton X-100, blocking with 10% goat serum for 1 hour, and incubation with the conjugated primary antibodies overnight at 4 °C. Staining of nuclei was performed using DAPI (10 μM for 7 min, Invitrogen, Waltham, MA).[32] After washing, all slides were mounted and preserved using ProLong Gold Antifade Mount (Invitrogen) before imaging *via* a confocal microscope (FV1000, Olympus, Tokyo, Japan) with FluoView software. ImageJ was used to quantify the ratio of area positive for each antibody relative to the area covered by DAPI.

Lipid profiling. Upon harvesting, fresh tissue biopsy samples (diameter of 1.5 mm), were snap frozen using a dry ice/isopentane slurry then subjected to liquid–liquid extraction using a modified Bligh & Dyer extraction method.[16] Samples were dried and concentrated (Eppendorf® Vacufuge™ 5a305) and stored at −80 °C until LC-MS/MS analysis. Before analyses, nonpolar samples (lipids) were reconstituted in 200 μl 1 : 1 MeOH : IPA (Fisher Chemical and Sigma Aldrich) and mixed and stored in 4 °C overnight. Samples were run in negative and positive mode on an Agilent 1290 Infinity II LC and 6545 MS System *via* a Waters Acquity UPLC HSS T3 column (1.8 μm, 2.1 × 150 mm) with attached guard column. MS/MS fragmentation of a pooled sample was performed *via* DDA acquisition at 10 V and 20 V for identification. The LC method consisted of a flow rate of 0.25 mL min^{-1} and a gradient of 0–2 min: 30% B; 17 min: 75% B; 20 min: 85% B; 23 min: 100% B; 26 min: 100% B; 27 min: 30% B. Solvent A: 60% acetonitrile, 40% water, 10 mM ammonium formate, 0.1% formic acid, 2.5 μM medronic acid. Solvent B: 90% isopropanol, 10% acetonitrile, 10 mM ammonium formate, 0.1% formic acid, 2.5 μM medronic acid. Identification was performed *via* Lipid Annotator to match MS/MS spectra. [M + H] or [M − H] adducts of all available lipid classes were analyzed, with a maximum 10 ppm mass error and minimum 90% total score. Features with multiple constituents were reported as the dominant species if relative abundance >10%. Peak areas were assigned using Skyline software.

Statistical analysis. Statistical analyses were performed *via* ANOVA with Fisher's *post-hoc* analysis, or Student t-tests where applicable, using Prism or Minitab statistical software. *p*-Values less than 0.05 were considered statistically significant. Letters show ranking of means and groups with the same letters are not statistically significant. Data are all presented as mean ± S.D. In figures where MACF and MAC groups are separated in two different graphs, the statistical analyses were performed on all groups as a whole and separation of groups is only for better visual comparison prioritizing MACF groups in the main manuscript and MAC in the ESI figures.†

Results and discussion

Hydrogel synthesis and characterization

MACF synthesis used a methacrylation reaction on chitosan (to make MAC) followed by fluorination of MAC. Fig. S1† details this reaction as well as the quantitative proton and fluorine NMR results to determine the degree of methacrylation (DM%, Fig. S1B†) and fluorine concentration (CF, Fig. S1C†) within MACF (26.28 ± 1%, and 90 ± 5 μM, respectively). These results indicated the successful incorporation of methacrylate and perfluorocarbon groups to the chitosan backbone, the latter being critical for oxygen transport enhancement properties. The appearance of the gels (Fig. 1A) shows changes in MAC's clear appearance changing to more of an opaque white colour in MACF.

Prior to beginning animal studies, we aimed to formulate the chitosan-based MACF/MAC hydrogel treatments with similar release kinetics of PHMB to the commercial Kendall-PHMB to ensure all treatments delivered similar PHMB to wounds. The Kendall dressing is FDA approved for topical treatment of infected wounds, thus Kendall's 0.5 wt% PHMB is generally considered safe for this purpose. Moreover, we have previously confirmed that this concentration of PHMB shows acceptable toxicity responses in HDFs in culture.[30,33] The results of this comparison demonstrated similar patterns of PHMB release for all three dressing types over the 72 hour course of study (Fig. 1B and C). The similar initial burst release for all dressings in the first 30 minutes of the release study is ideal for our application to allow early and rapid local accumulation of the antiseptic at the heavily infected wounds to eliminate bacteria. The steady release profile for the next 28 hours also aligned well with clinically recommended dressing change timepoints during our animal studies, which should be performed every 48–72 hours.[34,35]

Next, rheological properties of MAC and MACF hydrogels were studied to ensure dressings' ability to maintain structural integrity while providing optimal conformability to wound contours for improved wound healing. The complex shear modulus G^* was calculated as the arithmetic mean of the

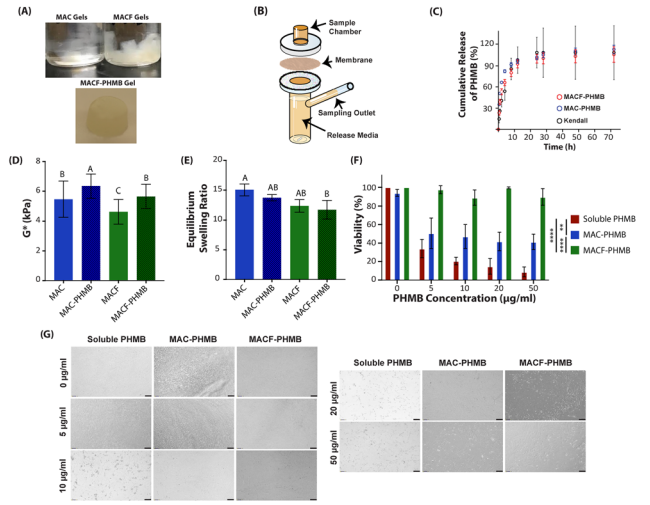

Fig. 1 (A) Visual differences between clear MAC and opaque MACF and MACF-PHMB hydrogels in their swollen state in PBS. (B) Franz cell schematic used for release studies. (C) *In vitro* release profiles of PHMB in PBS from MACF, MAC and commercial PHMB dressing substrates using standard Franz diffusion cells (Franz cell schematic recreated from PermeGear, Hellertown, PA, USA). Data mean ± cumulative S.D. (n = 3). Average mass of encapsulated PHMB was 400 μg, 133.1 μg and 410.5 μg for MACF-PHMB, Kendall, and MAC-PHMB, respectively. (D) Rheological properties of MAC and MACF hydrogels. Data n = 3; mean ± SD; significance determined by one-way ANOVA with Fisher's *post-hoc* (p < 0.0001). (E) Equilibrium swelling ratios of MAC and MACF hydrogels in PBS at 24 h, showing the ability of both hydrogels to absorb fluids around 11–15 times their initial dry state. Data all mean ± SD, n = 3. Statistical significance determined using one-way ANOVA with Fisher's *post-hoc* (p = 0.0159). (F) Viability of HDFs determined using PrestoBlue assay at different time points post direct contact with MAC and MACF hydrogels with PHMB, showing over 85% viability of the cells with MACF delivery of maximum PHMB dose (50 μg mL^{-1}) after 72 h. Data normalized to no-gel controls. Data all mean ± SD, with n = 3. Statistics using three-way ANOVA with Fisher's *post-hoc* analysis, (p < 0.05). (G) Morphological assessment of HDFs post 72 h of contact with MAC and MACF hydrogels with or without PHMB as compared to a non-treated control showing no visible differences in cell morphology.

storage modulus (G') and loss modulus (G'') allowing for stiffness comparisons of hydrogels (a higher G^* value corresponds to a stiffer gel).[36] As shown in Fig. 1D, MACF hydrogels had lower G^* values as compared to MAC. However, the slightly lowered stiffness did not affect MACF's handing efficiency when used as a wound dressing. Interestingly, PHMB incorporation did increase mechanical properties slightly for both MACF and MAC (p < 0.0001).

Liquid absorption is another critical factor to consider for wound dressings, especially when dealing with highly exudating wounds, such as infected wounds.[34,35] Swelling studies of MAC and MACF over 48 hours showed the ability of all tested hydrogel types to retain liquids 11–15 times greater than their initial dry state (Fig. 1E). There was no detected significance in the liquid absorption properties of the hydrogels with or without PHMB (p > 0.05).

Finally, *in vitro* cytotoxicity screening was performed on HDFs to study toxicity responses to the MAC and MACF base hydrogels, as well as the impact of adding PHMB at increasing concentrations. We used PrestoBlue colorimetric assay to quantitatively measure and compare cell viability within our different treatments.[37,38] Results of the PrestoBlue assay at equilibrium (72 hours of direct contact with both hydrogels) showed that soluble PHMB alone severely impacted viability, even at the lowest concentration (5 μg mL^{-1}). However, MACF treatment reversed toxicity with over 85% viability at the highest concentration of PHMB (50 μg mL^{-1}) in MACF (p < 0.0001 *vs.* soluble PHMB, Fig. 1F), while maintaining healthy cell morphologies (Fig. 1G). Cytotoxic impact of released PHMB was also minimized with application of MAC compared to free PHMB in media (p < 0.005), but significantly lower than MACF (p < 0.0001).

Considering the direct contact of our hydrogels with the wound for a minimum of 48 hours, it was crucial to evaluate their impact on skin cell viability. Our *in vitro* cytotoxicity assays with direct PHMB contact to HDFs, showed that MACF effectively reduced cytotoxic impacts of PHMB on cell viability (Fig. 1F and G), likely due to the impacts of oxygen on increasing metabolic processes of fibroblasts.[39] Although our tested concentrations were lower than the encapsulated concentrations for *in vivo* application, we chose to incorporate the same initial concentration of PHMB (0.5 wt%; Fig. 1C) as in the FDA-approved Kendall-PHMB dressing, since previous reports suggested acceptable host cell toxicity in multiple similar formulations, including PHMB foam and silicone dressings.[40] Although incorporating 0.5% PHMB in our hydrogels hypothetically means that the total amount of PHMB released could exceed 10 mg mL^{-1} locally, the actual bioavailable concentration of PHMB is much lower at every timepoint *in vivo*, which further supports our *in vitro* model. Also, wounds exudates, fluid circulation, drug degradation by host cells and bacteria, and the controlled release properties of our hydrogels, constantly dilute and inactivate a large portion of PHMB from the wound.[41–43]

Swelling properties of hydrogels were assessed due to their importance in maintaining wound moisture and enhancing healing processes.[44] Results (Fig. 1E) suggested that dressings utilizing MACF or MAC were able to absorb high levels of liquids which implies their ability to draw bacteria away from the wounds by entrapping wound fluids and bacteria. Interestingly, incorporation of PHMB only slightly decreased MAC and MACF swelling properties, likely due to PHMB interactions with the crosslinked chitosan backbones.[45] Swelling results lead to a recommendation for replacing MAC and MACF dressings every 48 hours *in vivo* to maintain exudate levels.

Wound treatments, size, morphology and histological evaluation

To assess the effectiveness of our treatments on wound healing in diabetic mice, we compared wound closure status on day 21 as a first readout (Fig. 2A, B and Fig. S6A, B† for MAC treatments). Our splinted wound model ensured that healing was achieved primarily through re-epithelialization

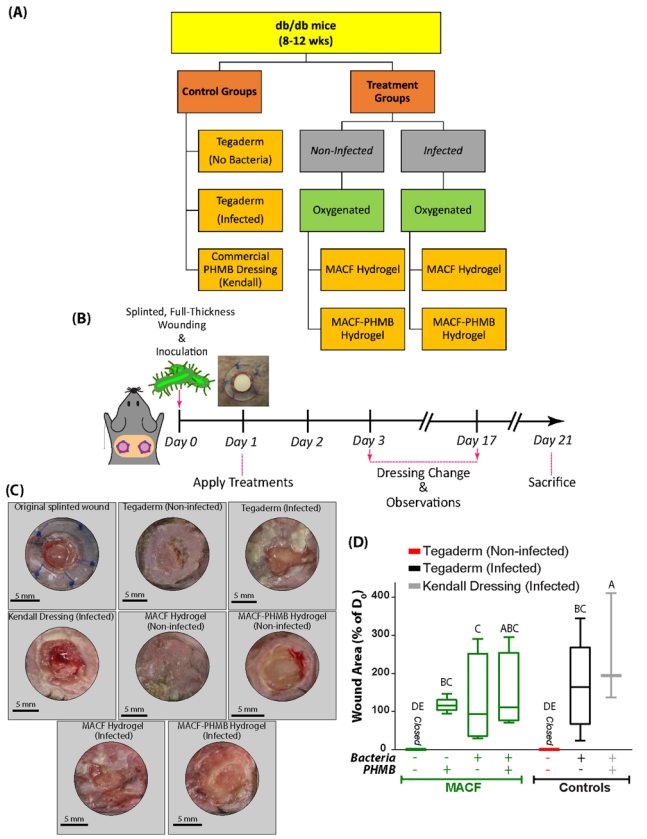

Fig. 2 Flow chart of treatments (A) and timeline (B) of the infected diabetic murine wound healing study. (C) Representative images of the wounds from day 0 and 21, showing obvious signs of infection and necrosis in groups infected with *P. aeruginosa*. (D) Wound area analyses from wound images on day 21 post-wounding (study endpoint) for treatment and control groups, showing a delayed wound healing response in all infected groups and successful wound closure in hydrogel-treated non-infected wounds. Data all mean ± S.D. from 3 to 5 biological samples. Significance by one-way ANOVA with Fisher's *post-hoc* test ($p < 0.05$).

and not contraction.[15–17] Successful establishment of infection in the groups inoculated with *P. aeruginosa* was observed, (Fig. 1C and Fig. S6†), and is supported by the large wound areas on day 21 in all infected groups (Fig. 2, $p < 0.03$) accompanied by visible bacterial accumulation marked by the green colour visible due to production of pyocyanin by *P. aeruginosa.*[46]

Interestingly, among all the groups that included PHMB (infected and non-infected), the commercial Kendall-PHMB dressing showed significantly larger wound areas as compared to hydrogel-PHMB groups (*i.e.*, MACF-PHMB and MAC-PHMB) ($p = 0.018$ Kendall *vs.* Tegaderm-only infected control) (Fig. 2C, D and Fig. S6†). Kendall dressings resulted in the largest wound areas on day 21 (247% increase as compared to the original wound). Furthermore, infected wounds treated with PHMB (regardless of dressing) on day 21 had a larger average area compared to the original wound area (day 0). Wound morphology and closure trends from day 7 and day 14 of the study shown in Fig. S2† support the trends seen at day 21 with uninfected MACF hydrogel treatments showing the fastest wound closure responses. Wound areas in the hydrogel groups were similar to the infected vehicle control ($p > 0.05$). Only the non-infected wounds treated with MACF, MAC, and Tegaderm successfully closed by day 21 of the study. These wound measurements revealed that the presence of bacteria, PHMB, or both prevented the wound from closing at this timepoint in all dressing treatments as well as the infected vehicle control (Tegaderm (infected), Fig. 2D). We did not observe any significant difference between the infected groups treated with MAC *vs.* MACF hydrogels ($p > 0.05$), suggesting no impact of additional oxygen *via* MACF hydrogels. Regardless of the type of treatment or infection status, all animals maintained their diabetic state throughout the experimental period as shown in Fig. S4.†

As part of this study, we aimed to examine potential sex differences in infected wound healing, as evidence from the literature suggests that host sex can potentially modulate wound healing responses,[39,45] where estrogen has been shown to speed up and regulate cutaneous healing.[39] To achieve this, we randomly selected from the pool of treatments (infected and non-infected) and controls shown in Fig. S4† and assigned them to male and female mice. Our results using wound area analysis demonstrated no significant differences in overall wound sizes in male and female diabetic *db*/*db* mice, regardless of the infection status or type of treatment used (Fig. S5,† $p > 0.05$). Thus, for the remainder of animal work we utilized male mice.

Next, histological assessments were performed in endpoint samples, which revealed tissue necrosis responses (as indicated by bright red areas over the wound bed in Masson's trichrome images) and disruption of the underlying collagen layer in all groups that were treated continuously with PHMB, including the commercial Kendall dressing treated wounds (Fig. 3 and Fig. S6C, D† for MAC treatments). We observed significantly longer epithelial tongues in the non-infected MACF-treated wounds as compared to the Tegaderm (non-infected) control (5.95 ± 0.54 mm *vs.* 2.67 ± 0.17 mm, respectively; $p = 0.0003$), suggesting improvement due to supplemental local oxygen from MACF; however, when infection and/or PHMB were present, no significant differences were observed independent of the type of treatment used ($p > 0.05$).

From the representative histology, and in agreement with our wound closure analyses, the presence of *P. aeruginosa* and PHMB substantially disrupted the wound healing process leading to necrosis responses (Fig. 3A). The infected wound groups all showed greatly expanded wound cross-sectional areas, with a disturbed or lacking granulation tissue (Fig. 2B). Interestingly, we did not observe any significant differences in the morphological and histological examinations resulting from the additional oxygenation delivered *via* MACF treatments compared to MAC (Fig. 2C and D, $p > 0.05$). This likely can be attributed to the low levels of additional local oxygen supplied by MACF treatments, as a material that continuously boosts local biological oxygen tensions by ~5–10 mmHg.[14]

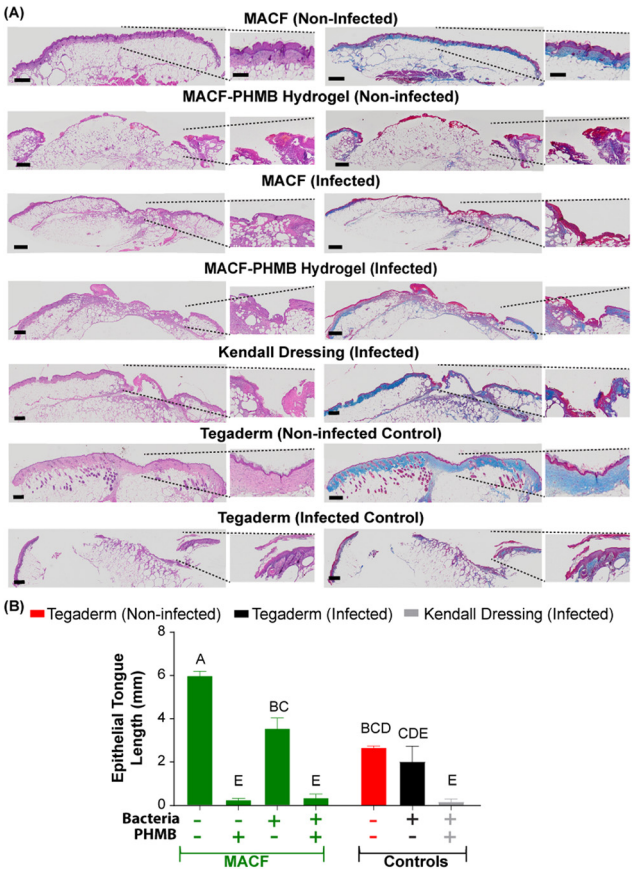

Fig. 3 (A) Wound histology assessment of day 21 wounds with H&E (left) and Masson's trichrome (right) staining. Scale bars are 500 μm and zoomed in images from the dotted portion is 5× larger. (B) Analysis of the length of epithelial tongue from histology images indicating the effect of bacteria and PHMB in creating wound bed necrotic regions as supported by shorter epithelial tongues in the infected hydrogel groups with or without PHMB. Data all mean ± S.D from 3 to 5 biological samples. Significance by one-way ANOVA with Fisher's *post hoc* test ($p < 0.05$).

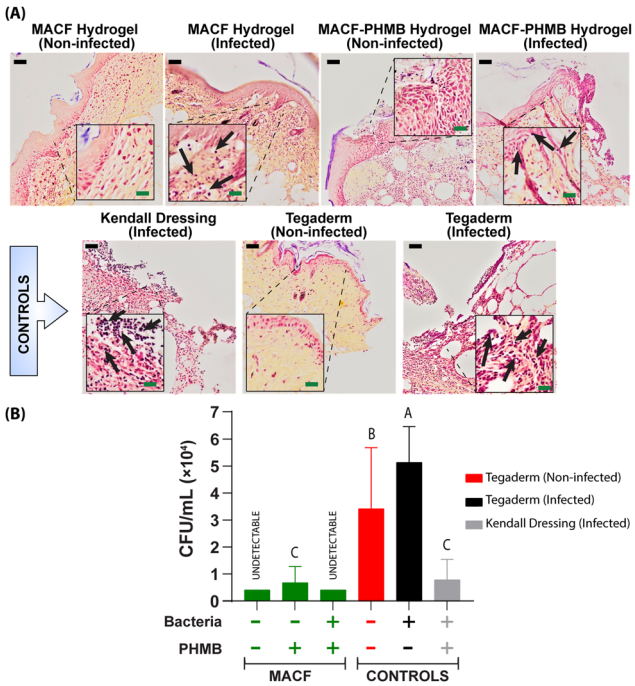

Fig. 4 (A) Representative tissue Gram-staining to visualize bacterial load and penetration at day 21. Black scale bars = 50 μm and green scale bars in zoom insets = 1.5 μm. Arrows indicate bacterial colonization. (B) Bacterial counts *via* qPCR from wound tissues harvested on day 21. Comparison between infected and non-infected wounds treated with MACF-based hydrogels showed significant reduction of *P. aeruginosa* in PHMB-treated infected wounds as compared to controls ($p < 0.05$). Treatments with no error bars indicate no amplification of *P. aeruginosa* 16S rRNA gene past designated cycle end, indicating no measurable presence of genomic DNA. Visible bars are due to calculation from maximum cycle number (C_T 35 representing no amplification) and are equivalent to zero bacterial load. Data $5 < n < 8$, mean ± S.D. Significance by one-way ANOVA with Fisher's *post-hoc* ($p < 0.05$).

This additional oxygenation may not be sufficient to upregulate host antibacterial responses, such as respiratory burst by circulating immune cells.[47] Conversely, the positive impacts of wound oxygenation on infection control have been reported previously when using systemic hyperbaric oxygen therapy (HBOT), which boost systemic oxygenation by over an atmosphere of pressure, leading to upregulated immune responses to infection.[19,21,48,49] Despite these observations there are other beneficial wound healing processes supplemental oxygenation for MACF could encourage as tied to oxidative cellular metabolic processes.[4,5,50]

Bacterial localization and quantification within the tissue

The degree of bacterial bioburden within wound tissues impacts wound healing responses, particularly in chronic wounds. Fig. 4 shows two analysis employed to better understand bacterial presence and load in endpoint samples. First, modified Gram staining of wound tissues harvested on day 21 revealed clusters of Gram-negative bacteria within the granulation tissue of the infected wounds, indicating deep-seated infection at the study endpoint. Despite the necrosis observed as associated with PHMB treatments, MACF-PHMB and MAC-PHMB groups exhibited remarkable reductions in bacterial loads compared to the Tegaderm (infected) control (Fig. 4A). In contrast, the group treated with the commercial Kendall-PHMB dressings showed uniformly dispersed populations of bacteria on day 21, indicating limited antibacterial action. Chitosan-based hydrogels, especially MACF-PHMB, performed better than the porous Kendall foam dressings in segregating bacteria. The depth of bacterial penetration in the MACF-PHMB and MAC-PHMB treated groups was improved, as evidenced by fewer bacteria in the deeper tissue layers compared to the Kendall dressing (Fig. 4A). During the study attempts to collect wound exudates *via* swabbing for conventional CFU counts proved to be challenging and unreliable due to the large variety and variability of natural flora on the wound. Thus, to confirm Gram-staining results and *P. aeruginosa* identity, whole wound tissues were subjected to CFU referenced qPCR assays (Fig. 4B). Infected Tegaderm con-

trols showed the highest *P. aeruginosa* CFU values, however, treatment with PHMB, either *via* MACF hydrogels or the commercial Kendall dressing, significantly reduced *P. aeruginosa* numbers ($p < 0.0027$) in day 21 samples. Importantly, MACF-PHMB hydrogel treatment rendered *P. aeruginosa* undetectable in both infected and non-infected groups.

P. aeruginosa localization deep in wounds in Gram-stained sections (Fig. 4A) of some infected treatments coincided with the lack of sufficient barrier function and the necrosis we observed in all infected groups at day 21 (Fig. 2B and 3A, B). Gjødsbøl *et al.*,[51] also reported *P. aeruginosa* localization in deeper wound regions associated with enlarged wound size and delayed wound healing. Conversely, our chitosan-based hydrogel-treated groups resulted more shallow bacterial penetration. This aligns with previous findings and emphasizes the impact of dressing choice on infection control. The confirmation of applied *P. aeruginosa* identity through qPCR at a higher titre than host wound flora further supports the effectiveness of PHMB in reducing loads of the strain within our treatment models (Fig. 4B). Undetectable levels of *P. aeruginosa* in MACF-PHMB group (infected and non-infected) definitively highlight its potential as a robust therapeutic option.

This initial animal study revealed a key finding that tissue necrosis and damage were caused by a combination of bacterial infection alongside continuous PHMB antiseptic treatment, regardless of dressing material. Antiseptics can elicit cytotoxic and inflammatory responses on host cellular contributors in wound healing process, such as keratinocytes, fibroblasts, and immune cells.[9] Consistently, a group[52] using *in vitro* scratch wound models showed a substantial reduction in fibroblast proliferation and migration when wounds were treated with hydrogen peroxide and povidone-iodine antiseptics. Notably, in their research, among all tested antiseptics, chlorhexidine (with similar structure to PHMB) was found to be one of the least toxic to fibroblasts.

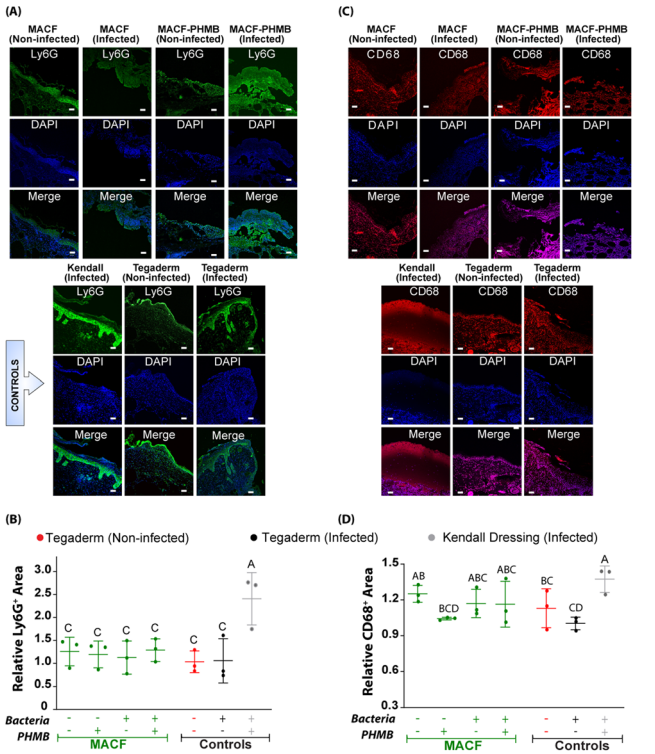

Fig. 5 (A) Neutrophil accumulation in the wound bed on day 21 as characterized by Ly6G staining. Green areas are positive for Ly6G, and blue shows nuclei staining using DAPI. Scale bars are 50 μm. (B) Quantitative analysis of the relative fluorescent area positive for Ly6G shows reduced levels of neutrophil accumulation in infected wounds treated with MACF hydrogels with or without PHMB, and similar to the commercial control dressing as compared to the infected control (+Bacteria/−PHMB). (C) Macrophage accumulation in the wound bed characterized by CD68 staining. Red areas are positive for CD68 and blue shows DAPI nuclei staining. Scale bars are 50 μm. (D) Quantitative analysis of the relative fluorescent area positive for CD68, which indicates significant accumulation of CD68+ macrophages on the top layer of infected wounds in Kendall dressing treated groups and a more uniform infiltration of these cells in all other treatment groups. Data all mean ± S.D from 3 to 5 biological samples. Significance by one-way ANOVA with Fisher's *post-hoc* ($p < 0.05$).

Leukocyte infiltration in wound tissues

For proper wound healing progression, neutrophils and their debris should exit the wound area to prevent chronic inflammation.[40] Thus, we examined the persistence of leukocytes at the wound site to better understand the state of wound healing. *Via* IHC and microscopy we observed the highest accumulation of Ly6G+ cells in infected wounds that were treated with the commercial Kendall dressing ($p = 0.0004$ *vs.* Tegaderm (infected)) (Fig. 5 and Fig. S9† for MAC treatments). The infiltration of neutrophils in the Kendall dressing group appeared to be more substantial through the epidermis layer and similar to the Tegaderm (infected) group. Other experimental groups, including Tegaderm (non-infected) control, MACF hydrogel, and MACF-PHMB hydrogel showed more uniform neutrophil populations throughout the tissue sections.

Inflammatory responses, such as infection and necrosis, are known to delay the process of neutrophil exit from wound sites.[53] When neutrophils persist in the wound site, they undergo apoptosis and release damaging metabolites causing further inflammation.[54] Accordingly, we observed significantly less neutrophils in infected wounds treated with MACF-PHMB groups as compared to MAC-PHMB treated infected wounds ($p = 0.02$) on day 21 (Fig. 5A and B). Supporting these results, a previous study reported decreased neutrophil adhesion to endothelial cells under elevated oxygen partial pressure conditions *via* HBOT *in vitro*.[49] This was correlated to reduced expression of endothelial intercellular adhesion molecule-1 as well as vascular cell adhesion molecule-1 mediated by *S*-nitrosation under HBOT. Similarly, another study observed a drastic decrease in adhesion-inducing cytokine β2-integrin expression of neutrophils under HBOT in patients with chronic non-healing wounds, confirming an anti-inflammatory role of oxygen.[50]

During wound healing, macrophages assist in the later stages of post-inflammation wound healing, playing important roles including phagocyting the remaining debris from the wound bed.[55] We did not observe any significant differences ($p > 0.05$) in macrophage distributions associated with any treatment used; however, a trend was observed in Kendall-PHMB treated infected group with the highest number of CD68+ (Fig. 5 and Fig. S9†) and CD11b+ cells (Fig. S10†). Our observations could be explained by the fact that the infected diabetic wounds remain trapped in an inflammatory phase, suggesting a non-healing state of the open wounds on day 21 could be tied to the extended presence of neutrophils and inflammation in the wound bed,[55] leading to a non-healing state in this wound model.

Effect of oxygenating antibacterial hydrogels on wound lipid profiles

Untargeted lipidomics provided a high throughput assessment of all experimental groups by showing that PHMB treatment, infection, and wound dressing altered levels of two key lipid classes, phosphatidylglycerols (PGs) and sphingomyelins (SMs) (Fig. 6), which are important for homeostatic skin physiology.[56,57] Treatment with MACF or MAC alone reduced levels of PG species when compared to all infected groups (Fig. 6 and Fig. S11† for MAC treatments). In contrast, PHMB delivery *via* MAC or MACF increased PG lipids within the treated wounds, in contrast to treatment *via* Kendall Dressing. Several SM species, including monounsaturated and polyunsaturated species, were increased by treatment with PHMB encapsulated in MACF and MAC, compared to both untreated, infected samples and those treated with Kendall dressings (Fig. 6 and Fig. S11†). While infection generally decreased the levels of lipids such as PGs and SMs, treatment with PHMB increased these levels. Interestingly, when PHMB was combined with MACF hydrogels, the infection-induced decrease was completely rescued.

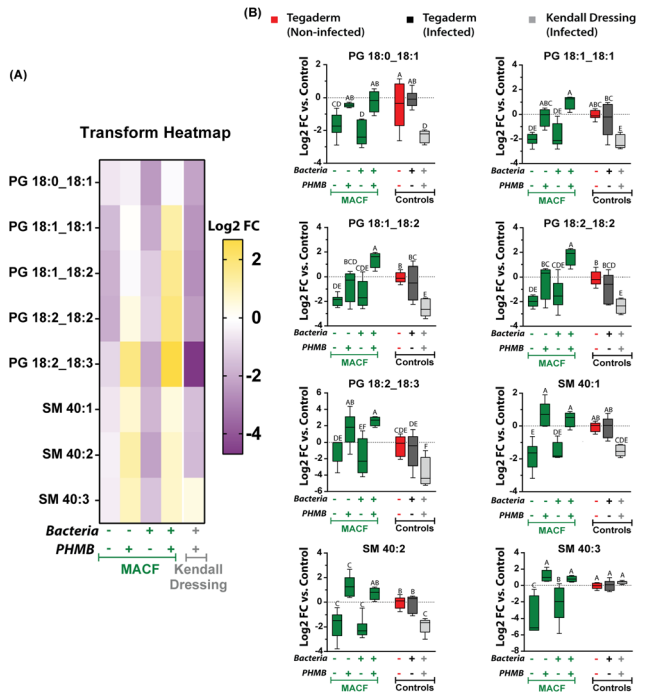

Fig. 6 Lipidomic profiling of infected diabetic wound healing on day 21. (A) Transform heatmap showing fold change of notable phosphatidylglycerols (PG) and sphingomyelins (SM). (B) Log fold change comparison of treatments *vs.* control (*i.e.,* Tegaderm (infected) for infected groups and Tegaderm (Non-infected) for non-infected). Trends indicate fold change decreases in multiple PGs and SMs when treated with Kendall dressing, whereas treatment with MACF showed similar profiles and even increases compared to negative controls. Significance by one-way ANOVA with Fisher's *post-hoc* test ($p < 0.05$) with $3 < n < 5$.

Here, we were interested in understanding the potential for lipidomics approaches to better understand wound healing responses in our infected diabetic wound model. Remarkably, MACF treatment stimulated increased levels of dioleoyl–PG (18 : 1/18 : 1) and dilinoleoyl–PG (18 : 2/18 : 2), both of which play a role in increasing keratinocyte proliferation (Fig. 6B). PGs are also known to modulate skin cell proliferation and promote anti-inflammatory responses.[56–58] Therefore, MACF-PHMB-mediated the regulation of the wound microenvironment and may optimize cell division in favour of wound closure. We also observed increased SM levels for the wounds treated with MACF-PHMB hydrogels (Fig. 6). These lipids play a critical role in maintaining the skin barrier and serve as precursors for signalling molecules, such as sphingosine-1-phosphate to induce keratinocyte differentiation and anti-apoptotic properties.[59,60] Wakita *et al.*[61] showed that sphingosylphosphorylcholine enhanced wound repair by directly stimulating keratinocyte migration and proliferation in diabetic mouse wound models. Overall, the initial lipid profiling results suggested that our hydrogel dressings can upregulate levels of SM and PG lipids despite the necrotic responses we observed *via* other analyses and enhance keratinocyte migration, proliferation, and differentiation, and inflammatory responses to encourage the restoration of dermal barrier functions. Apart from these two lipid types that showed most significant differences within our treatment groups, the entire raw data profile for all recognized lipids is available as ESI.†

Wound healing outcomes with reduced duration of PHMB application

Despite the positive effects of PHMB in clearing wound infection with our hydrogel treatments, the cumulative data (Fig. 1–5) suggested that the continuous application of this antiseptic over the 21-day study prolonged necrosis, inhibited the formation of epithelial and granulation layers, and may have led to chronic inflammation. Thus, we designed an additional study to determine if reducing the total length of PHMB exposure could improve wound re-epithelialization outcomes, while maintaining antibacterial actions. We divided animals into three groups: A. Animals infected with *P. aeruginosa* and treated with MACF-PHMB for 7 days then switched to plain oxygenating MACF hydrogels on day 7 to day 21 (no PHMB beyond D7); B. Animals with 14 days of MACF-PHMB treatment switched to plain oxygenating MACF

hydrogels on day 14 to day 21 (no PHMB beyond D14); C. Animals given continuous PHMB-MACF treatment for 21 days. Control data from the earlier studies were included for key comparisons (Fig. 7A). Gram-stained tissues at the 21-day endpoint showed deeper permeation and bacterial load in infected wounds treated with PHMB for only 7 days, as compared to 14 or 21 days (Fig. 7B). The qPCR data confirmed this finding, as infected wounds treated with PHMB for only 7 days showed greater load of *P. aeruginosa*, while treatment with PHMB for 14 and 21 days on infected wounds showed no measurable *P. aeruginosa* increase (Fig. 7C). Compared to data from our first animal study (Fig. 4), untreated infection controls showed higher loads of bacteria. Continuous Kendall PHMB treatment concerningly showed persistence of *P. aeruginosa* in wounds (Fig. 7C). We then compared the wound areas and epithelialization state of the two new PHMB MACF treatment groups *versus* the results from the continuous application of PHMB for 21 days. Histological observations revealed denser granulation tissue structures and improved epithelial tonguing in no PHMB beyond day 7, MACF oxygenated treatment for 14 days prior, especially in the non-infected PHMB treatment group (Fig. 7D and Fig. S12†). Wound area measurements in our non-infected groups revealed the positive impacts when PHMB was stopped at an earlier timepoint, since there were significant size differences of non-infected wounds ($p < 0.05$, Fig. S1†). However, the deleterious impact of bacteria on the infected wounds inhibited the complete wound healing process even when PHMB treatment concluded at an earlier timepoint (Fig. S10C† (infected groups)). The lipidomics studies (Fig. 7E) confirmed that wounds that experienced PHMB delivery through MACF showed overall upregulated SM and PG levels, with the highest levels observed on day 7. This observation, plus the lowest level of these lipids in the continuous PHMB treatment group, confirms the detrimental effects of prolonged tissue contact with PHMB in tissue repair processes, and supports the need to limit exposure of PHMB for treating wound infections.

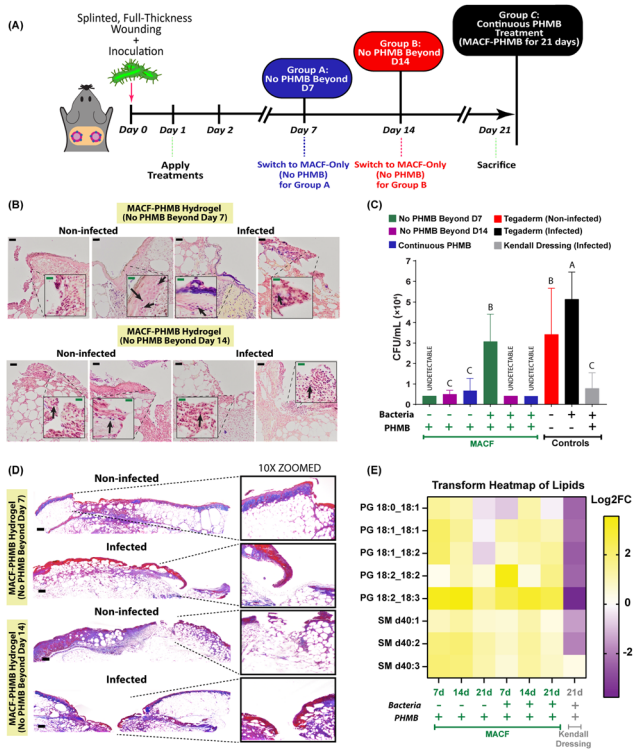

Fig. 7 (A) Design of experiment and timeline for assessing the effects of stopping PHMB delivery at two different midpoints, 7 and 14 days, as compared to continuous PHMB delivery for 21 days. (B) Representative tissue Gram-staining to study bacterial load and penetration at day 21 in treatment groups with highest load of bacteria corresponding to infected control and Kendall dressing groups. Black scale bars are 50 μm and green inset scale bars are 1.5 μm. Arrows indicate bacterial colonization. (C) Bacterial counts *via* qPCR from wound tissues harvested on day 21, treatments with MACF and PHMB up to day 14 and 21 reduced *P. aeruginosa* load well below non-infected Tegaderm only controls. Treatments with no error bars show no amplification of *P. aeruginosa* 16S rRNA gene past designated cycle end (cycle 35), indicating no measurable presence of genomic DNA. Data $5 < n < 8$, mean ± S.D. Significance by one-way ANOVA with Fisher's *post-hoc* ($p < 0.05$). (D) Representative wound histology Masson's trichrome staining. Scale bars are 500 μm. (E) Effect of stopping PHMB treatment at two different timepoints on lipid levels from wound extracts in infected and non-infected groups using lipid chromatography mass spectrometry ($3 < n < 5$) showing significant differences in lipid profiles when PHMB is used for 7 and 14 days *vs.* continuous application for 21 days (fold changes are calculated based on Tegaderm (infected) for infected groups and Tegaderm (non-infected) for non-infected).

Conclusions

In this study, we developed and evaluated oxygenating chitosan-based antibacterial hydrogel dressings for infected diabetic wound healing and compared the outcomes to a commercial foam antiseptic dressing (Kendall-PHMB). As the platform for our study, we created a wound model in *db*/*db* mice and infected them with *P. aeruginosa* to obtain a chronic bacterial infection in non-healing wounds. Despite the matched PHMB release kinetics of dressing treatments, our synergistic dual functioning MACF hydrogel dressings containing PHMB

antiseptic showed enhanced wound closure outcomes compared to the commercial Kendall-PHMB dressing. Persistence of neutrophils in the wound bed demonstrated that hydrogel dressings with supplemental oxygen *via* MACF attenuated inflammatory responses compared to their non-oxygenating (MAC) and foam dressing (Kendall) counterparts. We also examined lipid profile regulation in different treatment groups and discovered that our hydrogel dressings upregulate the levels of two important lipids classes of phosphatidylglycerols and sphingomyelins, which are known improve keratinocyte differentiation, reduce inflammatory responses, and restore skin barrier functions. Our oxygenating antibacterial chitosan-based hydrogel dressing, MACF-PHMB, consistently outperformed commercial Kendall foam dressings in our studies. This highlights the crucial role of dressing material choice in supporting host tissue regeneration and minimizing toxicity from the antiseptic PHMB. Despite these positive results, we observed problematic tissue necrosis with prolonged PHMB application. To address this, we refined our treatment strategy to apply PHMB only until the infection ceased, focusing on wound healing thereafter. Thus, our proposed healing strategy involves a 14-day PHMB application *via* our hydrogels, followed by plain MACF hydrogel treatment to achieve full wound closure and to encourage granulation tissue maturation and regeneration. We suggest future studies with endpoints longer than 21 days to capture the wound closure timepoints for each treatment group, once the infection is completely resolved. While recognizing the significance of directly measuring local wound oxygen levels to validate our hydrogel treatments and assess their impact on wound healing and anti-infective processes, it is crucial to acknowledge that existing oxygen sensors lack the sensitivity and resolution needed for precise topical oxygen measurements *in vivo*. Challenges include the need to anesthetize animals to ensure motionlessness during measurements, which can influence tissue oxygen dynamics and potentially skew results. Future efforts should prioritize development of new oxygen monitoring technologies for real-time monitoring of wound oxygenation states.

Overall, our designed antibacterial oxygenating hydrogels show strong promise for future translation as a multifunctional dressing for managing infected non-healing diabetic ulcers.

Abbreviations

AAALAC	Association for assessment and accreditation of laboratory animal care
AMP	Antimicrobial peptide
ANOVA	Analysis of variance
ATCC	American type culture collection
CFU	Colony-forming unit
d-TFA	Deuterated trifluoroacetic acid
D_2O	Deuterium oxide
DMEM	Dulbecco's modified Eagle's medium
DNA	Deoxyribonucleic acid
E. coli	*Escherichia coli*
ECM	Extracellular matrix
FBS	Foetal bovine serum
HDF	Human dermal fibroblasts
H&E	Hematoxylin and eosin
HBOT	Hyperbaric oxygen therapy
HEPA	High efficiency particulate air
HPLC	High-performance liquid chromatography
IACUC	Institutional animal care and use committee
IHC	Immunohistochemistry
IPA	Isopropyl alcohol
KDa	Kilodaltons
MAC	Methacrylamide chitosan
MACF	Fluorinated methacrylamide chitosan
MIC	Minimum inhibitory concentration
MS	Mass spectrometry
MMP	Matrix metalloproteinase
MWCO	Molecular weight cutoff
NIH	National institute of health
NMR	Nuclear magnetic resonance
OD	Optical density
OLAW	Office of laboratory animal welfare
P. aeruginosa	*Pseudomonas aeruginosa*
PBS	Phosphate-buffered saline
PFA	Paraformaldehyde
PFOC	Pentadecafluorooctanoyl chloride
PG	Phosphatidylglycerol
PHMB	Polyhexamethylene biguanide
qPCR	Quantitative polymerase chain reaction
ROS	Reactive oxygen species
RPMI	Roswell park memorial institute medium
S. aureus	*Staphylococcus aureus*
S.D	Standard deviation
SM	Sphingomyelin
TPA	12-*O*-Tetradecanoylphorbol-13-acetate
UV	Ultraviolet

Conflicts of interest

There are no conflicts to declare.

Acknowledgements

The authors would like to acknowledge the financial support for this research provided by the National Institute of Arthritis and Musculoskeletal and Skin Diseases (NIAMS, R21AR074743). The content of this publication reflects the views of the authors only and not NIAMS or NIH.

References

1 Z. Lin, T. Wu, W. Wang, B. Li, M. Wang, L. Chen, H. Xia and T. Zhang, *Int. J. Biol. Macromol.*, 2019, **140**, 330–342.

2 T. Tokatlian, C. Cam and T. Segura, *Adv. Healthc. Mater.*, 2015, **4**, 1084–1091.
3 J. He, Y. Qiao, H. Zhang, J. Zhao, W. Li, T. Xie, D. Zhong, Q. Wei, S. Hua, Y. Yu, K. Yao, H. A. Santos and M. Zhou, *Biomaterials*, 2020, **234**, 119763.
4 V. Skrypko, *J. Pharm. Innovation*, 2018, **7**, 1–2.
5 T. O. Kharchenko, O. K. Melekhovets, I. V. Melekhovets, A. S. Radko, N. V. Kalashnyk and R. S. N. Shu, *Problems of Endocrine Pathology*, 2020, **72**, 74–80.
6 B. A. Lipsky and C. Hoey, *Clin. Infect. Dis*, 2009, **49**, 1541–1549.
7 R. E. Hancock and D. P. Speert, *Drug Resistance Updates*, 2000, **3**, 247–255.
8 A. Punjataewakupt, S. Napavichayanun and P. Aramwit, *Eur. J. Clin. Microbiol. Infect. Dis.*, 2019, **38**, 39–54.
9 B. S. Atiyeh, S. A. Dibo and S. N. Hayek, *Int. Wound J.*, 2009, **6**, 420–430.
10 R. Smith, J. Russo, J. Fiegel and N. Brogden, *Antibiotics*, 2020, **9**, 56.
11 H. Chen, Y. Cheng, J. Tian, P. Yang, X. Zhang, Y. Chen, Y. Hu and J. Wu, *Sci. Adv.*, 2020, **6**, eaba4311.
12 E. Blackman, C. Moore, J. Hyatt, R. Railton and C. Frye, *Ostomy Wound Manage.*, 2010, **56**, 24–31.
13 J. P. Jee, R. Pangeni, S. K. Jha, Y. Byun and J. W. Park, *Int. J. Nanomed.*, 2019, **14**, 5449–5475.
14 P. S. Patil, M. Mansouri and N. D. Leipzig, *Adv. Biosyst.*, 2020, **4**, e1900250.
15 P. S. Patil, M. M. Evancho-Chapman, H. Li, H. Huang, R. L. George, L. P. Shriver and N. D. Leipzig, *PLoS One*, 2018, **13**, e0203371.
16 P. S. Patil, N. Fountas-Davis, H. Huang, M. Evancho-Chapman, J. A. Fulton, L. P. Shriver and N. D. Leipzig, *Acta Biomater.*, 2016, **36**, 164–174.
17 P. S. Patil, S. Fathollahipour, A. Inmann, A. Pant, R. Amini, L. P. Shriver and N. D. Leipzig, *Adv. Wound Care*, 2019, **8**, 374–385.
18 P. A. Shiekh, A. Singh and A. Kumar, *Biomaterials*, 2020, **249**, 120020.
19 M. Y. Memar, M. Yekani, N. Alizadeh and H. B. Baghi, *Biomed. Pharmacother.*, 2019, **109**, 440–447.
20 A. A. Tandara and T. A. Mustoe, *World J. Surg.*, 2004, **28**, 294–300.
21 C. J. Lerche, L. J. Christophersen, M. Kolpen, P. R. Nielsen, H. Trøstrup, K. Thomsen, O. Hyldegaard, H. Bundgaard, P. Jensen, N. Høiby and C. Moser, *Int. J. Antimicrob. Agents*, 2017, **50**, 406–412.
22 M. A. Kohanski, D. J. Dwyer, B. Hayete, C. A. Lawrence and J. J. Collins, *Cell*, 2007, **130**, 797–810.
23 A. Moeini, P. Pedram, P. Makvandi, M. Malinconico and G. Gomez d'Ayala, *Carbohydr. Polym.*, 2020, **233**, 115839.
24 S. Torkaman, H. Rahmani, A. Ashori and S. H. M. Najafi, *Carbohydr. Polym.*, 2021, **258**, 117675.
25 P. S. Patil and N. D. Leipzig, *J. Biomed. Mater. Res., Part A*, 2017, **105**, 2368–2374.
26 S. Fathollahipour, P. S. Patil and N. D. Leipzig, *Cells Tissues Organs*, 2018, **205**, 350–371.
27 T. R. Ham, D. D. Pukale, M. Hamrangsekachaee and N. D. Leipzig, *Mater. Sci. Eng., C*, 2020, **110**, 110656.
28 M. Hamrangsekachaee, H. J. Baumann, D. D. Pukale, L. P. Shriver and N. D. Leipzig, *ACS Appl. Bio Mater.*, 2022, **5**, 2176–2184.
29 U. Holzgrabe, *Prog. Nucl. Magn. Reson. Spectrosc.*, 2010, **57**, 229–240.
30 S. Abri, A. A. Ghatpande, J. Ress, H. A. Barton and N. D. Leipzig, *ACS Appl. Bio Mater.*, 2019, **2**, 5848–5858.
31 S. C. Becerra, D. C. Roy, C. J. Sanchez, R. J. Christy and D. M. Burmeister, *BMC Res. Notes*, 2016, **9**, 216.
32 D. D. Pukale, M. Farrag and N. D. Leipzig, *PLoS One*, 2021, **16**, e0252559.
33 J. Andrade Del Olmo, J. M. Alonso, V. Sáez-Martínez, S. Benito-Cid, I. Moreno-Benítez, M. Bengoa-Larrauri, R. Pérez-González, J. L. Vilas-Vilela and L. Pérez-Álvarez, *Biomater. Adv.*, 2022, **139**, 212992.
34 E. W. Group, *Int. Wound J.*, 2008, **5**, iii-19.
35 A. Novak, W. S. Khan and J. Palmer, *Open Orthop. J*, 2014, **8**, 168–177.
36 C. H. Wang, J. H. Cherng, C. C. Liu, T. J. Fang, Z. J. Hong, S. J. Chang, G. Y. Fan and S. D. Hsu, *Int. J. Mol. Sci.*, 2021, **13**, 7067.
37 P. F. Hsieh, C. C. Yu, P. M. Chu and P. L. Hsieh, *Antioxidants*, 2021, **10**, 1445.
38 N. Sianipar, Y. Hadisaputri, K. Assidqi, P. Simanjuntak and R. Purnamaningsih, *Rasayan J. Chem.*, 2020, **13**, 1992–1998.
39 M. S. Nakazawa, B. Keith and M. C. Simon, *Nat. Rev. Cancer*, 2016, **16**, 663–673.
40 C. B. Shah, H. P. Swaniker, B. J. Dowd, B. Brandon and D. A. Hibbitt, *Covidien*, 2009, **10**, 1–8.
41 W. Jin, P. Song, Y. Wu, Y. Tao, K. Yang, L. Gui, W. Zhang and F. Ge, *ACS Biomater. Sci. Eng.*, 2022, **8**, 4274–4288.
42 M. Burnet, D. G. Metcalf, S. Milo, C. Gamerith, A. Heinzle, E. Sigl, K. Eitel, M. Haalboom and P. G. Bowler, *Diagnostics*, 2022, **12**, 2408.
43 N. Pajares-Chamorro, Y. Wagley, N. Hammer, K. Hankenson and X. Chatzistavrou, *J. Am. Ceram. Soc.*, 2022, **105**, 1778–1789.
44 V. Brumberg, T. Astrelina, T. Malivanova and A. Samoilov, *Biomedicines*, 2021, **9**, 1235.
45 L. Pan, C. Li, Z. Wang, L. Yang and L. Zhang, *Biochem. Eng. J.*, 2022, **187**, 108626.
46 L. Allen, D. H. Dockrell, T. Pattery, D. G. Lee, P. Cornelis, P. G. Hellewell and M. K. Whyte, *J. Immunol.*, 2005, **174**, 3643–3649.
47 A. Ohta, *Int. Immunol.*, 2018, **30**, 335–343.
48 A. J. Almzaiel, R. Billington, G. Smerdon and A. J. Moody, *Life Sci.*, 2013, **93**, 125–131.
49 A. C. Kendall, J. L. Whatmore, P. G. Winyard, G. R. Smerdon and P. Eggleton, *Wound Repair Regener.*, 2013, **21**, 860–868.
50 M. Baiula, R. Greco, L. Ferrazzano, A. Caligiana, K. Hoxha, D. Bandini, P. Longobardi, S. Spampinato and A. Tolomelli, *PLoS One*, 2020, **15**, e0237746.

51 K. Gjødsbøl, J. J. Christensen, T. Karlsmark, B. Jørgensen, B. M. Klein and K. A. Krogfelt, *Int. Wound J.*, 2006, **3**, 225–231.
52 G. W. Thomas, L. T. Rael, R. Bar-Or, R. Shimonkevitz, C. W. Mains, D. S. Slone, M. L. Craun and D. Bar-Or, *J. Trauma*, 2009, **66**, 82–90; discussion 90-81.
53 A. R. Witter, B. M. Okunnu and R. E. Berg, *J. Immunol.*, 2016, **197**, 1557–1565.
54 J. Wang, *Cell Tissue Res.*, 2018, **371**, 531–539.
55 C. Murdoch, M. Muthana and C. E. Lewis, *J. Immunol.*, 2005, **175**, 6257–6263.
56 D. Xie, M. Seremwe, J. G. Edwards, R. Podolsky and W. B. Bollag, *PLoS One*, 2014, **9**, e107119.
57 W. M. Holleran, Y. Takagi and Y. Uchida, *FEBS Lett.*, 2006, **580**, 5456–5466.
58 V. Choudhary, R. Uaratanawong, R. R. Patel, H. Patel, W. Bao, B. Hartney, E. Cohen, X. Chen, Q. Zhong, C. M. Isales and W. B. Bollag, *J. Invest. Dermatol.*, 2019, **139**, 868–877.
59 L. Japtok, W. Bäumer and B. Kleuser, *Allergo J. Int.*, 2014, **23**, 54–59.
60 S. Borodzicz, L. Rudnicka, D. Mirowska-Guzel and A. Cudnoch-Jedrzejewska, *Lipids Health Dis.*, 2016, **15**, 1–9.
61 H. Wakita, Y. Tokura, H. Yagi, K. Nishimura, F. Furukawa and M. Takigawa, *Arch. Dermatol. Res.*, 1994, **286**, 350–354.